frontiers in Built Environment

ORIGINAL RESEARCH
published: 31 July 2018
doi: 10.3389/fbuil.2018.00038

Torsional Response Induced by Lateral Displacement and Inertial Force

Masayuki Kohiyama and Hiroki Yokoyama*

Department of System Design Engineering, Keio University, Yokohama, Japan

Eccentric distribution of stiffness, damping, and mass of a structure, and spatially non-uniform ground motion input to a long or large base mat of a structure are well-known causes of torsional response. We have discovered that the torque generated by horizontal displacement and perpendicular inertial force, which we call the Q-Δ effect, can be a cause of torsional response. We formulated the equation of motion of a single finite-size mass-linear elastic shear and torsion spring model and clarified the resonance condition of the torsional response to sinusoidal ground acceleration. Time-history response analysis verified that the torsional response forms beat and the maximum torsional response of the simulation result agrees with that theoretically predicted. Further time-history response analysis conducted of white noise ground acceleration showed that even one-directional white noise ground acceleration can induce torsional response in a linear elastic system without any structural eccentricity.

Keywords: torsional response, *Q*-*Δ* effect, geometric nonlinearity, large displacement, lateral force, high-rise building

OPEN ACCESS

Edited by:
Arturo Tena-Colunga, Universidad Autónoma Metropolitana, Mexico

Reviewed by:
Luigi Di Sarno, University of Sannio, Italy
George C. Tsiatas, University of Patras, Greece

***Correspondence:**
Masayuki Kohiyama
kohiyama@sd.keio.ac.jp

Specialty section:
This article was submitted to Earthquake Engineering, a section of the journal Frontiers in Built Environment

Received: *24 March 2018*
Accepted: *29 June 2018*
Published: *31 July 2018*

Citation:
Kohiyama M and Yokoyama H (2018) Torsional Response Induced by Lateral Displacement and Inertial Force. Front. Built Environ. 4:38. doi: 10.3389/fbuil.2018.00038

INTRODUCTION

Although torsional response induced by seismic ground motion has been investigated for more than 60 years, several factors still remain unclarified (Anagnostopoulos et al., 2015). As causes of the torsional response of buildings, researchers have studied eccentric distribution of stiffness (Georgoussis, 2009; Stathi et al., 2015), damping (Goel, 2000; Lin and Tsai, 2007), and the mass of a structure (Chandler and Hutchinson, 1986), in addition to spatially non-uniform or torsional ground motion input (De la Llera and Chopra, 1994; Heredia-Zavoni and Barranco, 1996; Basu and Giri, 2015; Falamarz-Sheikhabadi and Ghafory-Ashtiany, 2015; Gičev et al., 2015). A comprehensive review article has also been written by Anagnostopoulos et al. (2015). Therefore, their target buildings in general have an irregular, asymmetric structural property for the former perspective, which includes accidental eccentricity due to non-structural component or structural damage, and a long or large base mat that can incur phase difference of input ground motion for the latter. A few studies have also been conducted on the torsional response of symmetric buildings. For example, Tso (1975), Antonelli et al. (1981), and Pekau and Syamal (1984) studied the induction of torsional motion in symmetric structures with nonlinearity in the force-displacement relation of the lateral resisting elements. Cao et al. (2016, 2017) investigated the effects of near-fault pulse-like ground motions using a soil-foundation-structure system. Karayannis and Naoum (2018) studied an exceptional cause, asymmetric pounding with an adjacent building.

On the other hand, there are different powerful streams of studies on the P-Δ effect and rocking vibration (e.g., Wynhoven and Adams, 1972; Jennings and Bielak, 1973; Veletsos and Meek, 1974; Rutenberg, 1982; Akiyama, 1984; Bernal, 1987; Wilson and Habibullah, 1987; Uetani and Tagawa, 1992; MacRae, 1994; Tremblay et al., 1999; Aschheim and Hernández-Montes, 2003; Moghadam and Aziminejad, 2004; Humar et al., 2006; Deierlein et al., 2010; Yu et al., 2015). The P-Δ effect is a non-negligible overturning moment generated by dead loads and large lateral displacement. Rocking vibration is also induced by the overturning moment owing to the horizontal seismic force (inertial force) and the large height from the foundation to the point where the force is applied, in addition to foundation rocking caused by soil–structure interaction and/or incoherent ground motion. Flores et al. (2018) studied the amplification of torsional response due to the geometric nonlinearity effect of the gravity load.

From this moment-generating mechanism, we can infer torsional moment induction due to large lateral displacement and perpendicular inertial force (**Figure 1**). Although it has never been given significant focus, this effect might cause serious response amplification for high-rise buildings, which have large displacement under seismic excitation. In particular, as Japan has a high risk of large-magnitude earthquakes, which tend to generate broadband long-duration ground motion, it is crucial that the resonance of high-rise buildings be considered.

In this paper, we investigate this overlooked phenomenon, namely the Q-Δ effect, using a single-mass elastic model. The Q represents lateral force, which is *querkraft* in German, as conventionally used in mechanics. First, we formulate the equation of motion to model this phenomenon. Then, we derive the theoretical solution of response under sinusoidal wave input and clarify the condition that large torsional response appears. Finally, based on the condition, we demonstrate that single-directional white noise ground motion causes resonance of torsional mode using time-history response analysis.

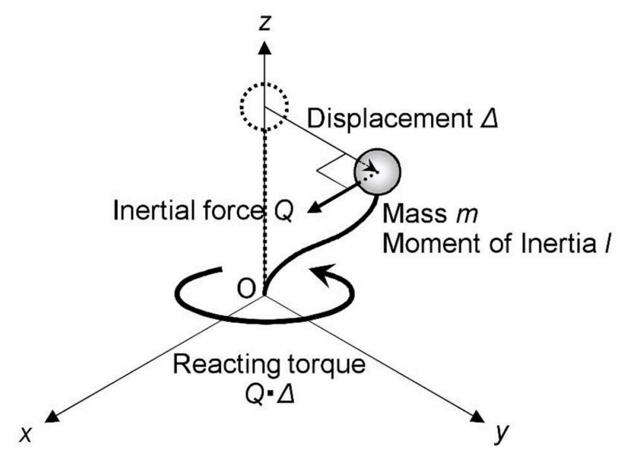

FIGURE 1 | Torque induced by lateral displacement and perpendicular inertial force.

DERIVATION OF CONDITIONS TO INDUCE TORSIONAL RESPONSE

Model and Equation of Motion

To investigate the fundamental principle of torsional response induction due to horizontal displacement and perpendicular inertial force, we utilize a single finite-size mass-linear elastic shear and torsion spring and damper model, which is an idealized model of a building, and derive the equation of motion under ground excitation. Here, we assume the linear elastic material property of columns, which is represented by a shear and torsion spring and damper, and geometric nonlinearity, i.e., large displacement of a floor slab, which is represented by a finite-size mass. **Figure 2** shows the model and the displacement variables used. Each rectangle represents a floor slab with a mass m and moment of inertia I. The horizontal displacement of the floor slab is represented by x and y in the x- and y-axis directions, respectively, and the rotation angle θ around the z axis in the anti-clockwise direction from the x axis. A column with horizontal shear stiffness k_x and k_y in the x- and y-axis direction, and k_θ for rotation around the z axis, connects the centroid G of the floor slab to the point O of the foundation on the ground surface. Similarly, we consider damping c_x, c_y, and c_θ between the floor slab and ground. That is, we model the story stiffness and damping with linear springs and viscous dampers of three degrees of freedom. Without loss of generality, we assume $k_x \geq k_y$. The system has the initial condition $(x, y, \theta) = (0, 0, 0)$ and $(\dot{x}, \dot{y}, \dot{\theta}) = (0, 0, 0)$ at time $t = 0$ and is subject to ground acceleration $(\ddot{x}_0, \ddot{y}_0, 0)$.

With respect to translational displacements, the equation of motion is described as follows:

$$-m\left(\ddot{x}_0 + \ddot{x}\right) - c_x\dot{x} - k_x x = 0 \tag{1}$$

$$\text{and } -m\left(\ddot{y}_0 + \ddot{y}\right) - c_y\dot{y} - k_y y = 0 \tag{2}$$

An inertial force perpendicular to the horizontal displacement generates a torsional moment M and its reaction moment $-M$ at ground (foundation of the structure) point O. We define M taking a positive value counterclockwise around the z axis. M is calculated as follows:

$$M = m\left(\ddot{x}_0 + \ddot{x}\right) y - m\left(\ddot{y}_0 + \ddot{y}\right) x \tag{3}$$

Alternatively, we can calculate the moment M in another manner. Horizontal reaction forces N_x and N_y in the x and y direction, which are supporting the column at point O, satisfy equilibrium with the restoring and damping forces of a column;

$$N_x = -c_x\dot{x} - k_x x \quad \text{and} \quad N_y = -c_y\dot{y} - k_y y \tag{4a, b}$$

Note that these reaction forces are the sum of non-conservative and conservative forces. These reaction forces at point O generate torsional moment M around the centroid G of the slab:

$$\begin{aligned} M &= N_x y - N_y x = \left(-c_x\dot{x} - k_x x\right) y - \left(-c_y\dot{y} - k_y y\right) x \\ &= -c_x\dot{x}y + c_y\dot{y}x - \left(k_x - k_y\right) xy \end{aligned} \tag{5}$$

If Equations (1) and (2) are substituted into Equation (5), we can confirm that Equation (5) is identical to Equation (3).

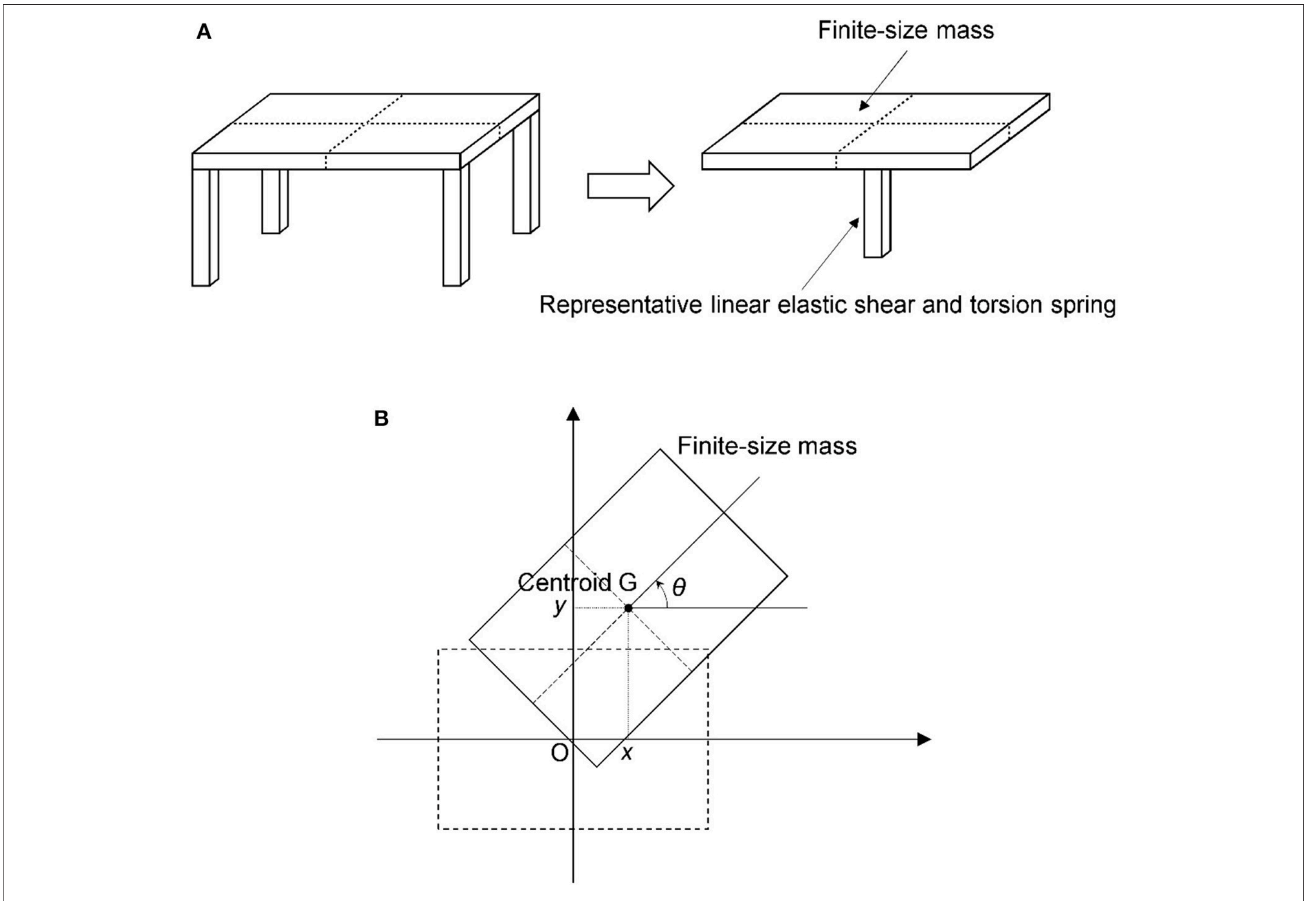

FIGURE 2 | A single finite-size mass–linear elastic shear and torsion spring model. **(A)** Representative linear elastic shear and torsion spring, **(B)** Displacement variables.

Using moment M, the equation of motion in the rotational direction is given as follows:

$$-I\ddot{\theta} - c_\theta\dot{\theta} - k_\theta\theta + M = 0 \tag{6}$$

We can summarize the equation of motion in matrices and vectors:

$$\begin{bmatrix} m & 0 & 0 \\ 0 & m & 0 \\ 0 & 0 & I \end{bmatrix} \begin{Bmatrix} \ddot{x} \\ \ddot{y} \\ \ddot{\theta} \end{Bmatrix} + \begin{bmatrix} c_x & 0 & 0 \\ 0 & c_y & 0 \\ 0 & 0 & c_\theta \end{bmatrix} \begin{Bmatrix} \dot{x} \\ \dot{y} \\ \dot{\theta} \end{Bmatrix} + \begin{bmatrix} k_x & 0 & 0 \\ 0 & k_y & 0 \\ 0 & 0 & k_\theta \end{bmatrix} \begin{Bmatrix} x \\ y \\ \theta \end{Bmatrix} = \begin{Bmatrix} -m\ddot{x}_0 \\ -m\ddot{y}_0 \\ M \end{Bmatrix} \tag{7}$$

In the above equation, torsional moment (torque) generated by the inertial force is in the right side and we can regard this torque as an external moment of seismic force and perpendicular displacement.

The equations of motion are transformed into the following vibration equations:

$$\ddot{x} + 2\zeta_x\omega_x\dot{x} + \omega_x^2 x = -\ddot{x}_0, \tag{8}$$

$$\ddot{y} + 2\zeta_y\omega_y\dot{y} + \omega_y^2 y = -\ddot{y}_0, \tag{9}$$

and
$$\begin{aligned} \ddot{\theta} + 2\zeta_\theta\omega_\theta\dot{\theta} + \omega_\theta^2\theta &= \frac{M}{I} \\ &= \frac{(\ddot{x}_0 + \ddot{x})\, y - \left(\ddot{y}_0 + \ddot{y}\right) x}{r_\theta^2} \\ &= \frac{-2\zeta_x\omega_x\dot{x}y + 2\zeta_y\omega_y\dot{y}x - \left(\omega_x^2 - \omega_y^2\right) xy}{r_\theta^2} \end{aligned} \tag{10}$$

where the natural circular frequencies

$$\omega_x = \sqrt{\frac{k_x}{m}},\ \omega_y = \sqrt{\frac{k_y}{m}},\ \text{and } \omega_\theta = \sqrt{\frac{k_\theta}{m}} \tag{11a, b, c}$$

damping factors

$$\zeta_x = \frac{c_x}{2\omega_x m} = \frac{c_x}{2\sqrt{k_x m}},\ \zeta_y = \frac{c_y}{2\omega_y m} = \frac{c_y}{2\sqrt{k_y m}},$$

$$\text{and } \zeta_\theta = \frac{c_\theta}{2\omega_\theta I} = \frac{c_\theta}{2\sqrt{k_\theta I}} \tag{12a, b, c}$$

and radius of gyration

$$r_\theta = \sqrt{\frac{I}{m}} = \sqrt{\frac{L_x^2 + L_y^2}{12}} \tag{13}$$

L_x and L_y represent the length of the floor slab in the x and y directions, respectively, and we assume the slab has uniform density. Because we assume $k_x \geq k_y$, natural frequencies in translational modes have the relation $\omega_x \geq \omega_y$.

Steady-State Response to Unit Complex Ground Acceleration

We input the following unit complex ground acceleration into the target system:

$$\ddot{x}_0 = \mathrm{e}^{\mathrm{i}p_x t} \quad \text{and} \quad \ddot{y}_0 = \mathrm{e}^{\mathrm{i}p_y t} \tag{14a, b}$$

where i is an imaginary unit, and p_x and p_y are circular frequencies of ground acceleration in the x and y directions, respectively. The vibrations of equations in the translational directions are mutually independent and we first focus on steady-state response in the x direction. The solution to response x can be assumed in the following form:

$$x = X\mathrm{e}^{\mathrm{i}p_x t} \tag{15}$$

where X represents the complex amplitude of the steady-state response in the x direction. By substituting this equation into Equation (8), we obtain

$$\left(-p_x^2 + 2\mathrm{i}p_x\zeta_x\omega_x + \omega_x^2\right) X\mathrm{e}^{\mathrm{i}p_x t} = -e^{\mathrm{i}p_x t} \tag{16}$$

Therefore, complex amplitude X is given by

$$X = \frac{-1}{-p_x^2 + 2\mathrm{i}p_x\zeta_x\omega_x + \omega_x^2} = |X|\,\mathrm{e}^{\mathrm{i}\phi_x} \tag{17}$$

where $|X|$ and ϕ_x represent the absolute value and phase of X:

$$|X| = \frac{1}{p_x^2}\frac{\left(\frac{p_x}{\omega_x}\right)^2}{\sqrt{\left\{1 - \left(\frac{p_x}{\omega_x}\right)^2\right\}^2 + 4\zeta_x^2\left(\frac{p_x}{\omega_x}\right)^2}} \tag{18}$$

$$\text{and } \phi_x = \arg\left[-\left\{1 - \left(\frac{p_x}{\omega_x}\right)^2\right\} + 2\mathrm{i}\zeta_x\left(\frac{p_x}{\omega_x}\right)\right] \tag{19}$$

In the same manner, the steady-state response in the y direction is obtained as follows:

$$y = Y\mathrm{e}^{\mathrm{i}p_y t}, \tag{20}$$

$$Y = |Y|\,\mathrm{e}^{\mathrm{i}\phi_y}, \tag{21}$$

$$|Y| = \frac{1}{p_y^2}\frac{\left(\frac{p_y}{\omega_y}\right)^2}{\sqrt{\left\{1 - \left(\frac{p_y}{\omega_y}\right)^2\right\}^2 + 4\zeta_y^2\left(\frac{p_y}{\omega_y}\right)^2}}, \tag{22}$$

$$\text{and } \phi_y = \arg\left[-\left\{1 - \left(\frac{p_y}{\omega_y}\right)^2\right\} + 2\mathrm{i}\zeta_y\left(\frac{p_y}{\omega_y}\right)\right] \tag{23}$$

With respect to the rotational direction, we first calculate M/I in Equation (10).

$$\begin{aligned}\frac{M}{I} &= \frac{(\ddot{x}_0 + \ddot{x})\,y - (\ddot{y}_0 + \ddot{y})\,x}{r_\theta^2} \\ &= \frac{\left(-e^{\mathrm{i}p_x t} - p_x^2 X e^{\mathrm{i}p_x t}\right) Y e^{\mathrm{i}p_y t} - \left(-e^{\mathrm{i}p_y t} - p_y^2 Y e^{\mathrm{i}p_y t}\right) X e^{\mathrm{i}p_x t}}{r_\theta^2} \\ &= \frac{\left\{-\left(1 + p_x^2 X\right) Y + \left(1 + p_y^2 Y\right) X\right\} \mathrm{e}^{\mathrm{i}\left(p_x + p_y\right)t}}{r_\theta^2} \\ &= \frac{\left\{X - Y - \left(p_x^2 - p_y^2\right) XY\right\} \mathrm{e}^{\mathrm{i}\left(p_x + p_y\right)t}}{r_\theta^2}\end{aligned} \tag{24}$$

Alternatively, we can obtain a simpler expression using Equation (10):

$$\begin{aligned}\frac{M}{I} &= \frac{-2\zeta_x\omega_x\dot{x}y + 2\zeta_y\omega_y\dot{y}x - \left(\omega_x^2 - \omega_y^2\right) xy}{r_\theta^2} \\ &= \frac{-2\zeta_x\omega_x\mathrm{i}p_x X\mathrm{e}^{\mathrm{i}p_x t} Y\mathrm{e}^{\mathrm{i}p_y t} + 2\zeta_y\omega_y\mathrm{i}p_y Y\mathrm{e}^{\mathrm{i}p_y t} X\mathrm{e}^{\mathrm{i}p_x t} - (\omega_x^2 - \omega_y^2) X\mathrm{e}^{\mathrm{i}p_x t} Y\mathrm{e}^{\mathrm{i}p_y t}}{r_\theta^2} \\ &= \frac{\left\{-2\mathrm{i}(\zeta_x\omega_x p_x - \zeta_y\omega_y p_y) - (\omega_x^2 - \omega_y^2)\right\} XY\mathrm{e}^{\mathrm{i}\left(p_x + p_y\right)t}}{r_\theta^2} \\ &= |A|\,\mathrm{e}^{\mathrm{i}\phi_a} XY\mathrm{e}^{\mathrm{i}\left(p_x + p_y\right)t} \\ &= XYA\mathrm{e}^{\mathrm{i}\left(p_x + p_y\right)t}\end{aligned} \tag{25}$$

where

$$|A| = \frac{\sqrt{\left(\omega_x^2 - \omega_y^2\right)^2 + 4\left(\zeta_x\omega_x p_x - \zeta_y\omega_y p_y\right)^2}}{r_\theta^2}, \tag{26}$$

$$\phi_a = \arg\left[-\left(\omega_x^2 - \omega_y^2\right) - 2\mathrm{i}(\zeta_x\omega_x p_x - \zeta_y\omega_y p_y)\right],$$

$$\text{and} \quad A = |A|\,\mathrm{e}^{\mathrm{i}\phi_a}, \tag{27a, b}$$

By substituting this solution into the rotational vibration Equation (10),

$$\ddot{\theta} + 2\zeta_\theta\omega_\theta\dot{\theta} + \omega_\theta^2\theta = XYA\mathrm{e}^{\mathrm{i}\left(p_x + p_y\right)t} \tag{28}$$

Because the system is linear also in the rotational direction, the steady-state rotational response under complex ground acceleration with a circular frequency of $p_x + p_y$ can be solved as follows:

$$\theta = XYA\Theta\mathrm{e}^{\mathrm{i}\left(p_x + p_y\right)t} = S\mathrm{e}^{\mathrm{i}\left(p_x + p_y\right)t} \tag{29}$$

where

$$\Theta = |\Theta|\, e^{i\phi_\theta}, \tag{30}$$

$$|\Theta| = \frac{1}{\left(p_x + p_y\right)^2} \frac{\left(\frac{p_x+p_y}{\omega_\theta}\right)^2}{\sqrt{\left\{1-\left(\frac{p_x+p_y}{\omega_\theta}\right)^2\right\}^2 + 4\zeta_\theta^2\left(\frac{p_x+p_y}{\omega_\theta}\right)^2}}, \tag{31}$$

$$\phi_\theta = \arg\left[-\left\{1-\left(\frac{p_x+p_y}{\omega_\theta}\right)^2\right\} + 2i\zeta_\theta\left(\frac{p_x+p_y}{\omega_\theta}\right)\right], \tag{32}$$

$$S = |S|\, e^{i\phi} = XYA\Theta, \tag{33}$$

$$|S| = |X||Y||A||\Theta|, \tag{34}$$

and

$$\phi = \phi_x + \phi_y + \phi_a + \phi_\theta \tag{35}$$

From this solution, it is clear that the torsional response has an amplitude proportional to that of the translational responses in two orthogonal directions and has a circular frequency of $p_x + p_y$; i.e., the summation of circular frequencies of ground acceleration in two orthogonal directions.

Derivation of Torsional Mode Resonance Condition Under Unit Complex Ground Acceleration

Suppose that the damping factors ζ_x and ζ_y are small, resonance of translational responses occur when ground acceleration circular frequency is identical to natural circular frequency:

$$p_x = \omega_x \quad \text{and} \quad p_y = \omega_y \tag{36a, b}$$

In this case, the response amplitudes are approximated as follows:

$$|X| \approx \frac{1}{p_x^2}\frac{1}{2\zeta_x} \text{ and } |Y| \approx \frac{1}{p_y^2}\frac{1}{2\zeta_y} \tag{37a, b}$$

Equation (26) is transformed as follows:

$$|A| = \frac{\sqrt{\left(\omega_x^2-\omega_y^2\right)^2 + 4\left(\zeta_x\omega_x^2 - \zeta_y\omega_y^2\right)^2}}{r_\theta^2} \tag{38}$$

Now, we introduce an assumption that damping factors are the same ζ in three directions:

$$\zeta_x = \zeta_y = \zeta_\theta = \zeta \tag{39}$$

Then, Equation (38) is transformed into

$$|A| = \frac{\sqrt{\left(\omega_x^2-\omega_y^2\right)^2 + 4\zeta^2\left(\omega_x^2-\omega_y^2\right)^2}}{r_\theta^2} = \frac{\sqrt{1+4\zeta^2}\,|\omega_x^2-\omega_y^2|}{r_\theta^2} \tag{40}$$

With respect to torsional response, Equations (31), (36a,b) give the resonance condition:

$$p_x + p_y = \omega_x + \omega_y = \omega_\theta \tag{41}$$

In this case, $|\Theta|$ is approximated as follows:

$$|\Theta| \approx \frac{1}{\left(p_x+p_y\right)^2}\frac{1}{2\zeta_\theta} = \frac{1}{\left(\omega_x+\omega_y\right)^2}\frac{1}{2\zeta} \tag{42}$$

Finally, the torsional response amplitude $|S|$ in the resonance state is given by

$$\begin{aligned}|S| &= |X|\,|Y|\,|A|\,|\Theta| \\ &= \frac{1}{8\zeta^3\omega_x^2\omega_y^2\left(\omega_x+\omega_y\right)^2}\frac{\sqrt{1+4\zeta^2}\,\left|\omega_x^2-\omega_y^2\right|}{r_\theta^2} \\ &= \frac{1}{8r_\theta^2}\frac{\sqrt{1+4\zeta^2}}{\zeta^3}\frac{\left|\omega_x-\omega_y\right|}{\omega_x^2\omega_y^2(\omega_x+\omega_y)}\end{aligned} \tag{43}$$

It should be noted that, when a system has the same natural circular frequency in two translational directions, i.e., $\omega_x = \omega_y$, torsional response is not induced because $|S|$ is zero.

If the resonance condition is rewritten by using system natural periods T_x, T_y, T_θ and ground motion period T_{0x}, T_{0y},

$$T_{0x} = T_x \quad \text{and} \quad T_{0y} = T_y \tag{44a, b}$$

$$\frac{1}{T_{0x}} + \frac{1}{T_{0y}} = \frac{1}{T_x} + \frac{1}{T_y} = \frac{1}{T_\theta} \tag{45}$$

where

$$T_x = \frac{2\pi}{\omega_x},\ T_y = \frac{2\pi}{\omega_y},\ T_\theta = \frac{2\pi}{\omega_\theta},\ T_{0x} = \frac{2\pi}{\omega_{0x}},\ \text{and } T_{0y} = \frac{2\pi}{\omega_{0y}} \tag{46a–e}$$

From Equation (45), we obtain

$$T_\theta = \frac{T_x T_y}{T_x + T_y} \tag{47}$$

Steady-State Response to Unit Sinusoidal Ground Acceleration

Next, we consider unit sinusoidal ground acceleration. The input ground motions are defined as follows:

$$\ddot{x}_0 = \sin p_x t = \frac{e^{ip_x t} - e^{-ip_x t}}{2i} \tag{48}$$

$$\ddot{y}_0 = \sin p_y t = \frac{e^{ip_y t} - e^{-ip_y t}}{2i} \tag{49}$$

where p_x and p_y are the circular frequency of the input sine waves. Steady-state translational responses are derived from the result of the unit complex ground acceleration case:

$$x = \mathrm{Im}\left(Xe^{ip_x t}\right) = |X|\sin\left(p_x t + \phi_x\right) = |X|\,\frac{e^{i(p_x t+\phi_x)} - e^{-i(p_x t+\phi_x)}}{2i} \tag{50}$$

$$y = \mathrm{Im}\left(Ye^{ip_y t}\right) = |Y|\sin\left(p_y t + \phi_y\right) = |Y|\,\frac{e^{i(p_y t+\phi_y)} - e^{-i(p_y t+\phi_y)}}{2i} \tag{51}$$

By taking the time derivatives of these equations, we obtain

$$\dot{x} = |X|\,\mathrm{i}p_x \frac{\mathrm{e}^{\mathrm{i}(p_x t+\phi_x)} + \mathrm{e}^{-\mathrm{i}(p_x t+\phi_x)}}{2\mathrm{i}} \tag{52}$$

$$\dot{y} = |Y|\,\mathrm{i}p_y \frac{\mathrm{e}^{\mathrm{i}(p_y t+\phi_y)} + \mathrm{e}^{-\mathrm{i}(p_y t+\phi_y)}}{2\mathrm{i}} \tag{53}$$

Using these equations, we can calculate the following products:

$$\begin{aligned}\dot{x}y &= -\frac{|X|\,|Y|\,\mathrm{i}p_x}{4}\left\{\mathrm{e}^{\mathrm{i}(p_x t+\phi_x)} + \mathrm{e}^{-\mathrm{i}(p_x t+\phi_x)}\right\}\left\{\mathrm{e}^{\mathrm{i}(p_y t+\phi_y)} - \mathrm{e}^{-\mathrm{i}(p_y t+\phi_y)}\right\}\\ &= \frac{|X|\,|Y|\,\mathrm{i}p_x}{4}\Big[-e^{\mathrm{i}\{(p_x+p_y)t+(\phi_x+\phi_y)\}} + \mathrm{e}^{-\mathrm{i}\{(p_x+p_y)t+(\phi_x+\phi_y)\}}\\ &\quad + \mathrm{e}^{\mathrm{i}\{(p_x-p_y)t+(\phi_x-\phi_y)\}} - \mathrm{e}^{-\mathrm{i}\{(p_x-p_y)t+(\phi_x-\phi_y)\}}\Big]\end{aligned} \tag{54}$$

$$\begin{aligned}\dot{y}x &= \frac{|X|\,|Y|\,\mathrm{i}p_y}{4}\Big[-e^{\mathrm{i}\{(p_x+p_y)t+(\phi_x+\phi_y)\}} + \mathrm{e}^{-\mathrm{i}\{(p_x+p_y)t+(\phi_x+\phi_y)\}}\\ &\quad - \mathrm{e}^{\mathrm{i}\{(p_x-p_y)t+(\phi_x-\phi_y)\}} + \mathrm{e}^{-\mathrm{i}\{(p_x-p_y)t+(\phi_x-\phi_y)\}}\Big]\end{aligned} \tag{55}$$

$$\begin{aligned}xy &= \frac{|X|\,|Y|}{4}\Big[-\mathrm{e}^{\mathrm{i}\{(p_x+p_y)t+(\phi_x+\phi_y)\}} - \mathrm{e}^{-\mathrm{i}\{(p_x+p_y)t+(\phi_x+\phi_y)\}}\\ &\quad +\mathrm{e}^{\mathrm{i}\{(p_x-p_y)t+(\phi_x-\phi_y)\}} + \mathrm{e}^{-\mathrm{i}\{(p_x-p_y)t+(\phi_x-\phi_y)\}}\Big]\end{aligned} \tag{56}$$

The right side of term M/I in Equation (10) is then calculated as follows:

$$\begin{aligned}\frac{M}{I} &= \frac{-2\zeta_x\omega_x\dot{x}y + 2\zeta_y\omega_y\dot{y}x - \left(\omega_x^2-\omega_y^2\right)xy}{r_\theta^2}\\ &= \frac{|X|\,|Y|}{4r_\theta^2}\Big[\left\{2\mathrm{i}(\zeta_x\omega_x p_x - \zeta_y\omega_y p_y) + \left(\omega_x^2-\omega_y^2\right)\right\}\mathrm{e}^{\mathrm{i}\{(p_x+p_y)t+(\phi_x+\phi_y)\}}\\ &\quad + \left\{-2\mathrm{i}(\zeta_x\omega_x p_x - \zeta_y\omega_y p_y) + \left(\omega_x^2-\omega_y^2\right)\right\}\mathrm{e}^{\mathrm{i}\{(p_x+p_y)t+(\phi_x+\phi_y)\}}\\ &\quad + \left\{-2\mathrm{i}(\zeta_x\omega_x p_x + \zeta_y\omega_y p_y) - \left(\omega_x^2-\omega_y^2\right)\right\}\mathrm{e}^{\mathrm{i}\{(p_x-p_y)t+(\phi_x-\phi_y)\}}\\ &\quad + \left\{2\mathrm{i}(\zeta_x\omega_x p_x + \zeta_y\omega_y p_y) - \left(\omega_x^2-\omega_y^2\right)\right\}\mathrm{e}^{\mathrm{i}\{(p_x-p_y)t+(\phi_x-\phi_y)\}}\Big]\\ &= \frac{|X|\,|Y|}{4}\Big[|A_1|\Big[\mathrm{e}^{\mathrm{i}\{(p_x+p_y)t+(\phi_x+\phi_y+\phi_{a1})\}} + \mathrm{e}^{\mathrm{i}\{(p_x+p_y)t+(\phi_x+\phi_y+\phi_{a1})\}}\Big]\\ &\quad + |A_2|\Big[\mathrm{e}^{\mathrm{i}\{(p_x-p_y)t+(\phi_x-\phi_y+\phi_{a2})\}} + \mathrm{e}^{\mathrm{i}\{(p_x-p_y)t+(\phi_x-\phi_y+\phi_{a2})\}}\Big]\Big]\\ &= \frac{|X|\,|Y|}{2}\Big[|A_1|\cos\{(p_x+p_y)t+(\phi_x+\phi_y+\phi_{a1})\}\\ &\quad + |A_2|\cos\{(p_x-p_y)t+(\phi_x-\phi_y+\phi_{a2})\}\Big]\\ &= \mathrm{Re}\left[\frac{|X|\,|Y|}{2}\Big[|A_1|\,\mathrm{e}^{\mathrm{i}\{(p_x+p_y)t+(\phi_x+\phi_y+\phi_{a1})\}}\right.\\ &\quad \left. + |A_2|\,\mathrm{e}^{\mathrm{i}\{(p_x-p_y)t+(\phi_x-\phi_y+\phi_{a2})\}}\Big]\right]\\ &= \mathrm{Re}\left[\frac{XY}{2}\left\{A_1\mathrm{e}^{\mathrm{i}\,(p_x+p_y)t} + A_2\mathrm{e}^{\mathrm{i}\,(p_x-p_y)t}\right\}\right]\end{aligned} \tag{57}$$

where

$$|A_1| = \frac{\sqrt{\left(\omega_x^2-\omega_y^2\right)^2 + 4\left(\zeta_x\omega_x p_x - \zeta_y\omega_y p_y\right)^2}}{r_\theta^2}, \tag{58}$$

$$\phi_{a1} = \arg\left[-\left(\omega_x^2-\omega_y^2\right) - 2\mathrm{i}(\zeta_x\omega_x p_x - \zeta_y\omega_y p_y)\right], \tag{59}$$

$$|A_2| = \frac{\sqrt{\left(\omega_x^2-\omega_y^2\right)^2 + 4\left(\zeta_x\omega_x p_x + \zeta_y\omega_y p_y\right)^2}}{r_\theta^2}, \tag{60}$$

$$\phi_{a2} = \arg\left[\left(\omega_x^2-\omega_y^2\right) + 2\mathrm{i}(\zeta_x\omega_x p_x + \zeta_y\omega_y p_y)\right], \tag{61}$$

$$A_1 = |A_1|\,\mathrm{e}^{\mathrm{i}\phi_{a1}}, \tag{62}$$

$$\text{and } A_2 = |A_2|\,\mathrm{e}^{\mathrm{i}\phi_{a2}} \tag{63}$$

Therefore, the rotational vibration equation is given by

$$\begin{aligned}&\ddot{\theta} + 2\zeta_\theta\omega_\theta\dot{\theta} + \omega_\theta^2\theta\\ &= \frac{|X|\,|Y|}{2}\Big[|A_1|\cos\{(p_x+p_y)t+(\phi_x+\phi_y+\phi_{a1})\}\\ &\quad + |A_2|\cos\{(p_x-p_y)t+(\phi_x-\phi_y+\phi_{a2})\}\Big]\\ &= \mathrm{Re}\left[\frac{XY}{2}\left(A_1\mathrm{e}^{\mathrm{i}\,(p_x+p_y)t} + A_2\mathrm{e}^{\mathrm{i}\,(p_x-p_y)t}\right)\right]\end{aligned} \tag{64}$$

Because the right side of Equation (64) is the real part of the summation of the complex external forces with two different circular frequencies, we can derive the torsional response in the same manner as in section Steady-State Response to Unit Complex Ground Acceleration:

$$\begin{aligned}\theta &= \mathrm{Re}[S_1\mathrm{e}^{\mathrm{i}\left(p_x+p_y\right)t} + S_2\mathrm{e}^{\mathrm{i}\left(p_x-p_y\right)t}]\\ &= |S_1|\cos\{\left(p_x+p_y\right)t+\phi_1\} + |S_2|\cos\{\left(p_x-p_y\right)t+\phi_2\}\end{aligned} \tag{65}$$

where

$$S_1 = |S_1|\,\mathrm{e}^{\mathrm{i}\phi_1} = \frac{XYA_1\Theta_1}{2}, \tag{66}$$

$$|S_1| = \frac{|X|\,|Y|\,|A_1|\,|\Theta_1|}{2}, \tag{67}$$

$$\phi_1 = \phi_x + \phi_y + \phi_{a1} + \phi_{\theta1}, \tag{68}$$

$$\Theta_1 = |\Theta_1|\,\mathrm{e}^{\mathrm{i}\phi_{\theta1}}, \tag{69}$$

$$|\Theta_1| = \frac{1}{\left(p_x+p_y\right)^2}\frac{\left(\frac{p_x+p_y}{\omega_\theta}\right)^2}{\sqrt{\left\{1-\left(\frac{p_x+p_y}{\omega_\theta}\right)^2\right\}^2 + 4\zeta_\theta^2\left(\frac{p_x+p_y}{\omega_\theta}\right)^2}}, \tag{70}$$

$$\phi_{\theta1} = \arg\left[-\left\{1-\left(\frac{p_x+p_y}{\omega_\theta}\right)^2\right\} + 2\mathrm{i}\zeta_\theta\left(\frac{p_x+p_y}{\omega_\theta}\right)\right], \tag{71}$$

$$S_2 = |S_2|\,\mathrm{e}^{\mathrm{i}\phi_2} = \frac{XYA_2\Theta_2}{2}, \tag{72}$$

$$|S_2| = \frac{|X|\,|Y|\,|A_2|\,|\Theta_2|}{2}, \tag{73}$$

$$\phi_2 = \phi_x + \phi_y + \phi_{a2} + \phi_{\theta2}, \tag{74}$$

$$\Theta_2 = |\Theta_2|\,\mathrm{e}^{\mathrm{i}\phi_{\theta2}}, \tag{75}$$

$$|\Theta_2| = \frac{1}{\left(p_x-p_y\right)^2}\frac{\left(\frac{p_x-p_y}{\omega_\theta}\right)^2}{\sqrt{\left\{1-\left(\frac{p_x-p_y}{\omega_\theta}\right)^2\right\}^2 + 4\zeta_\theta^2\left(\frac{p_x-p_y}{\omega_\theta}\right)^2}}, \tag{76}$$

$$\text{and } \phi_{\theta2} = \arg\left[-\left\{1-\left(\frac{p_x-p_y}{\omega_\theta}\right)^2\right\} + 2\mathrm{i}\zeta_\theta\left(\frac{p_x-p_y}{\omega_\theta}\right)\right] \tag{77}$$

Equation (65) can be described in a different way:

$$\begin{aligned}\theta &= \mathrm{Re}\left[\frac{XY}{2}\left\{A_1\Theta_1 e^{\mathrm{i}\left(p_x+p_y\right)t} + A_2\Theta_2 e^{\mathrm{i}\left(p_x-p_y\right)t}\right\}\right]\\ &= \frac{|X||Y|}{2}\Big[|A_1||\Theta_1|\cos\{\left(p_x+p_y\right)t+\phi_1\}\\ &\quad + |A_2||\Theta_2|\cos\{\left(p_x-p_y\right)t+\phi_2\}\Big] \qquad (78)\end{aligned}$$

We observe that torsional response is proportional to the amplitude of the translational response in two orthogonal directions and its form is the superposition of two sine waves with circular frequencies $p_x + p_y$ and $p_x - p_y$. This is easily understood because the ground acceleration consists of complex ground accelerations with circular frequencies of p_x and $-p_x$ in the x direction and p_y and $-p_y$ in the y direction. Further, on the basis of Equation (29), the torsional response is given by the combination of two circular frequencies in the orthogonal directions; i.e., $\pm(p_x + p_y)$ and $\pm(p_x - p_y)$.

Derivation of Torsional Mode Resonance Condition Under Sinusoidal Ground Acceleration

To determine the condition of torsional mode resonance under sinusoidal ground acceleration, we assume that the damping factors are small and the translational mode resonance is occurring in two directions owing to the ground acceleration frequency being identical to the natural circular frequency:

$$p_x = \omega_x \quad \text{and} \quad p_y = \omega_y \qquad (79\text{a, b})$$

The amplitudes of the translational responses can be approximated as follows:

$$|X| \approx \frac{1}{p_x^2}\frac{1}{2\zeta_x} \quad \text{and} \quad |Y| \approx \frac{1}{p_y^2}\frac{1}{2\zeta_y}. \qquad (80\text{a, b})$$

Using the following formula:

$$\begin{aligned}& a_1\cos(\omega_1 t+\phi_1) + a_2\cos(\omega_2 t+\phi_2)\\ &= a_1\cos(\omega_1 t+\phi_1)\\ &\quad + a_2\cos[(\omega_1 t+\phi_1) - \{(\omega_1 t+\phi_1)-(\omega_2 t+\phi_2)\}]\\ &= [a_1 + a_2\cos\{(\omega_1 t+\phi_1)-(\omega_2 t+\phi_2)\}]\cos(\omega_1 t+\phi_1)\\ &\quad + a_2\sin\{(\omega_1 t+\phi_1)-(\omega_2 t+\phi_2)\}\sin(\omega_1 t+\phi_1)\\ &= \sqrt{a_1^2 + a_2^2 + 2a_1a_2\cos\{(\omega_1-\omega_2)t+\phi_1-\phi_2\}}\\ &\quad \times \cos(\omega_1 t+\phi_1+\alpha) \qquad (81)\end{aligned}$$

where α is an additional phase introduced by calculation of trigonometric functions, the right side of Equation (78) can be transformed as follows:

$$\begin{aligned}& |A_1||\Theta_1|\cos\{\left(p_x+p_y\right)t+\phi_1\} + |A_2||\Theta_2|\cos\{\left(p_x-p_y\right)t+\phi_2\}\\ &= \sqrt{|A_1|^2|\Theta_1|^2 + |A_2|^2|\Theta_2|^2 + 2|A_1||A_2||\Theta_1||\Theta_2|\cos\left(2p_y t+\phi_1-\phi_2\right)}\\ &\quad \times \cos\{\left(p_x+p_y\right)t+\phi_1+\alpha\} \qquad (82)\end{aligned}$$

The result implies that the torsional response is a beat, of which amplitude changes periodically. The maximum amplitude is estimated by

$$|\theta_{\max}| = |S_1| + |S_2| = \frac{|X||Y|}{2}(|A_1||\Theta_1| + |A_2||\Theta_2|) \qquad (83)$$

Here, we introduce another assumption that the damping factors are identical:

$$\zeta_x = \zeta_y = \zeta_\theta = \zeta \qquad (84)$$

Then, Equations (58) and (60) are simplified as follows:

$$\begin{aligned}|A_1| &= \frac{\sqrt{\left(\omega_x^2-\omega_y^2\right)^2 + 4\zeta^2\left(\omega_x^2-\omega_y^2\right)^2}}{r_\theta^2}\\ &= \frac{\sqrt{1+4\zeta^2}\left|\omega_x^2-\omega_y^2\right|}{r_\theta^2} \qquad (85)\end{aligned}$$

$$\text{and } |A_2| = \frac{\sqrt{\left(\omega_x^2-\omega_y^2\right)^2 + 4\zeta^2\left(\omega_x^2+\omega_y^2\right)^2}}{r_\theta^2} \qquad (86)$$

This result suggests that large torsional response occurs when the difference between two natural frequencies of orthogonal translational modes is large. In addition, $|A_1| < |A_2|$ because $\omega_x > 0$ and $\omega_y > 0$.

Equations (70) and (76) with respect to $|\Theta_1|$ and $|\Theta_2|$ give alternative conditions of torsional mode resonance as follows:

$$\begin{aligned}\omega_\theta &= p_x + p_y = \omega_x + \omega_y = \omega_{\theta+}\\ \text{or } \omega_\theta &= p_x - p_y = \omega_x - \omega_y = \omega_{\theta-} \qquad (87\text{a, b})\end{aligned}$$

Equations (87a,b) correspond to the resonance conditions of the first and second terms in Equation (83), respectively. To distinguish these two natural circular frequencies to cause resonance, we name the former and latter $\omega_{\theta+}$ and $\omega_{\theta-}$, respectively.

If the condition is rewritten using natural periods,

$$\begin{cases} T_{0x} = T_x \\ T_{0y} = T_y \\ T_\theta = T_{\theta+} = \frac{T_xT_y}{T_x+T_y} \text{ or } T_\theta = T_{\theta-} = \frac{T_xT_y}{-T_x+T_y} \end{cases} \qquad (88\text{a–d})$$

where

$$T_x = \frac{2\pi}{\omega_x},\ T_y = \frac{2\pi}{\omega_y},\ T_\theta = \frac{2\pi}{\omega_\theta},\ T_{0x} = \frac{2\pi}{\omega_{0x}},\ \text{and } T_{0y} = \frac{2\pi}{\omega_{0y}} \qquad (89\text{a–e})$$

VERIFICATION BASED ON NUMERICAL SIMULATION

Simulation of Response to Sinusoidal Ground Acceleration

Large torsional response due to resonance is predicted when the natural period of torsional mode satisfies Equations (88c)

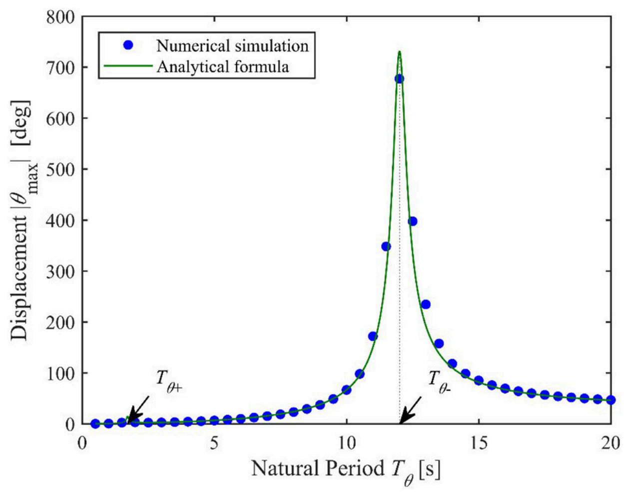

FIGURE 3 | Relation between the maximum displacement of torsional response $|\theta_{\max}|$ and the natural period of torsional mode T_θ.

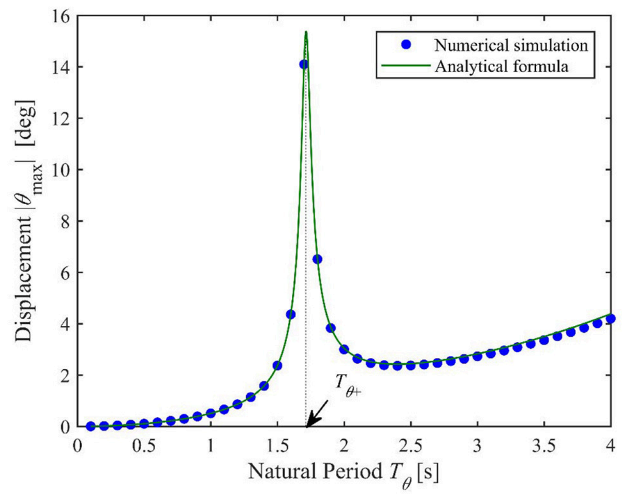

FIGURE 4 | Zoomed-up graph for the range 0 s $\leq T_\theta \leq$ 4 s.

or (88d) and two orthogonal translational modes also cause resonance. We verify this prediction via numerical simulation below.

We use a model with $T_x = T_{0x} = 3.00$ s, $T_y = T_{0y} = 4.00$ s, $\zeta = 2.00 \times 10^{-2}$, and $r_\theta = 20.0$ m. The estimated maximum torsional response of Equation (83) can be rewritten as a function of $T_\theta = 2\pi/\omega_\theta$:

$$|\theta_{\max}(T_\theta)| = \frac{|X||Y|}{2}\left(|A_1|\left|\Theta_1(T_\theta)\right| + |A_2|\left|\Theta_2(T_\theta)\right|\right) \quad (90)$$

Because of the assumption that translational modes cause resonance, the values of $|X|$ and $|Y|$ are calculated using Equations (80a,b). Equations (85) and (86) indicate that $|A_1|$ and $|A_2|$ are independent of ω_θ; i.e., T_θ. Therefore, the relation between the estimated maximum displacement of torsional response $|\theta_{\max}|$ and natural period of torsional mode T_θ can be depicted as the green curve in **Figure 3**.

From Equations (88c,d), the torsional response causes resonance when $T_\theta = T_{\theta+} = 1.71$ s or $T_{\theta-} = 12.0$ s. Therefore, the condition Equation (88d) gives quite a larger response. However, when looking at a database of natural periods of actual existing buildings (Architectural Institute of Japan., 2000), the natural period of torsional mode, T_θ, is generally smaller than that of the translational modes, T_x and T_y. To check the detail of the period range of 0 to 4 s, **Figure 4** shows a zoomed-up graph. At this range, condition (88c) gives the largest maximum response.

The time-history analysis of vibration Equations (8–10) are conducted by using the Newmark β method with the parameter $\beta = 1/6$ and time step interval $\Delta t = 0.01$ s. We first conduct time integration of Equations (8, 9). Then, the torsional response is calculated by using the obtained translational responses.

TABLE 1 | Parameter values for numerical simulation.

Parameter	Value	Parameter	Value
T_x	3.00 s	A_{0x}	1.00 m/s^2
T_y	4.00 s	A_{0y}	1.00 m/s^2
T_θ	1.71 s	T_{0x}	3.00 s
ζ	2.00×10^{-2}	T_{0y}	4.00 s
r_θ	20.0 m		

Input ground accelerations are given by the following sine waves:

$$\ddot{x}_0 = A_{0x} \sin\left(\frac{2\pi}{T_{0x}}t\right) \quad \text{and} \quad \ddot{y}_0 = A_{0y} \sin\left(\frac{2\pi}{T_{0y}}t\right) \quad (91\text{a, b})$$

The parameters of the target model and ground accelerations are shown in **Table 1**, in which T_θ is determined based on the resonance condition of torsional mode, Equations (88a–c).

Figure 5A shows input ground motion and **Figure 5B** the simulated displacement response. The response gradually shifts to a steady state. We can verify that the torsional response (red line in **Figures 5B,C**) shapes a beat and the maximum response matches the theoretically predicted value of 15.4° shown in **Figure 4**.

To examine the validity of Equation (90), other models with a different T_θ value were simulated and the maximum responses in a duration of 300 s recorded. The results for $T_\theta \in$ [0.5 s, 1 s, 1.5 s, ..., 20 s] are shown by blue points in **Figure 3**. Similarly, the results for $T_\theta \in$ [0.1 s, 0.2 s, 0.3 s, ..., 4 s] are shown in **Figure 4**. The numerical simulation results are virtually identical to the predicted values.

Simulation of Response to White Noise Ground Acceleration

Seismic ground motion is often modeled by filtered white noise. White noise, which has a flat power spectrum over all frequencies, can excite translational modes with any natural

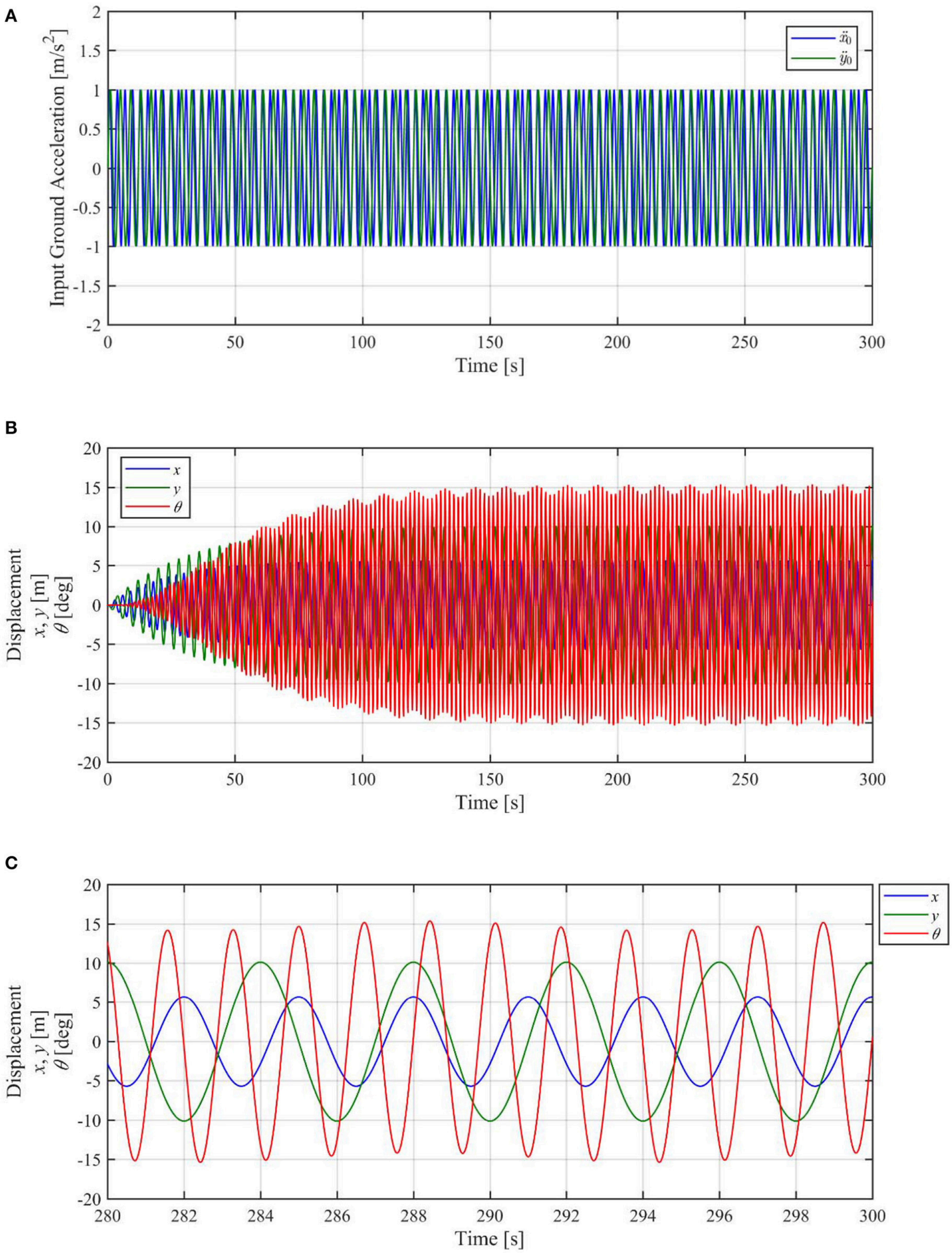

FIGURE 5 | Time-history analysis result of displacement response to sinusoidal ground acceleration. **(A)** Input ground motion, **(B)** Displacement response, **(C)** Displacement response (zoomed-up graph).

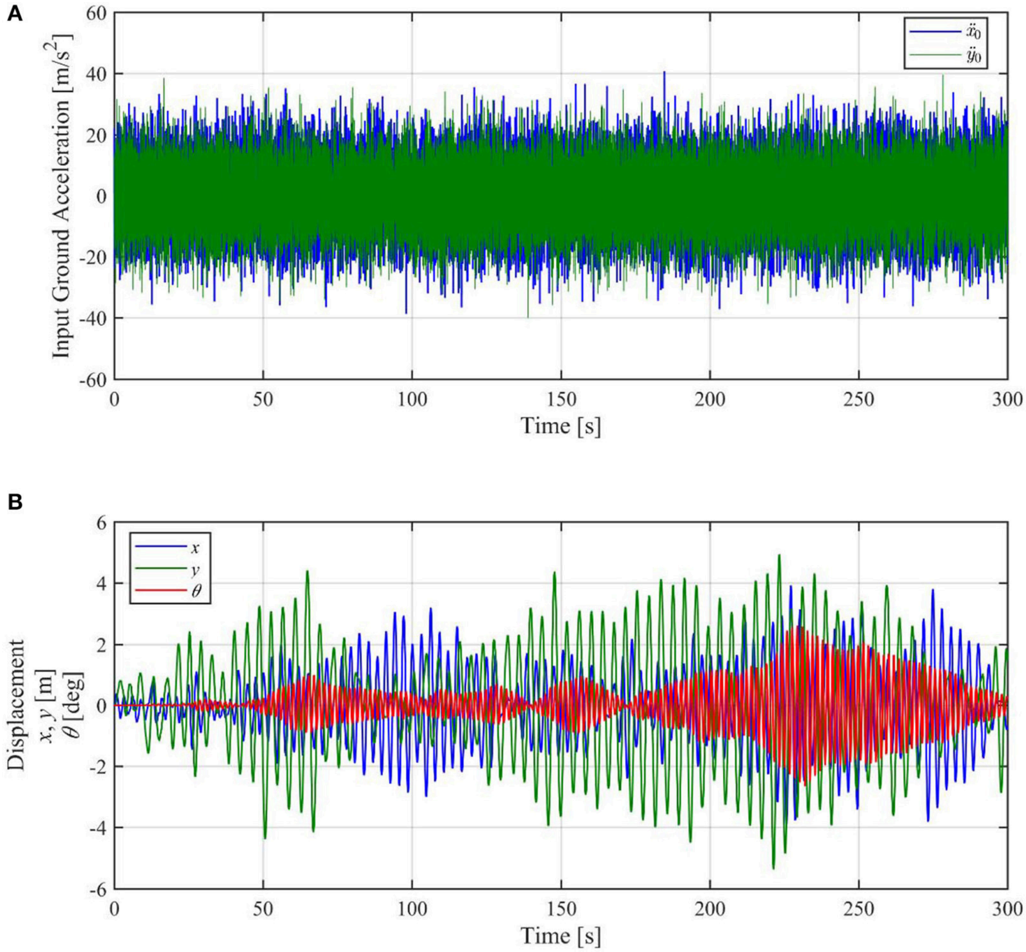

FIGURE 6 | Time-history analysis result of displacement response to uncorrelated two-directional white noise ground acceleration. **(A)** Input ground acceleration **(B)** Displacement response.

frequency. Therefore, it could excite two orthogonal translational modes with different natural frequencies and consequently could induce torsional response. We first input uncorrelated white noise ground accelerations in the x and y directions, as shown in **Figure 6A**. The power spectrum density of both accelerations is $S_{x0} = S_{y0} = 1.00$ m^2/s^3. **Figure 6B** shows the simulation results. It can be seen that the torsional response (red line) is induced by uncorrelated two-directional white noise ground acceleration.

Next, we input fully correlated white noise ground accelerations in the x and y directions in the same manner, as shown in **Figure 7A**. This is equivalent to inputting one-directional white noise ground acceleration in the 45° direction from the x axis. The power spectrum density of the accelerations is $S_{x0} = S_{y0} = 0.707$ m^2/s^3; i.e., 1.00 m^2/s^3 in the excitation direction. The result is shown in **Figure 7B**, where it can be seen that the maximum torsional response exceeds 2.0° under the used input ground acceleration. We thus confirm that even one-directional ground motion can induce the torsional response of a symmetric structure without any eccentricity.

CONCLUSIONS

In past studies, researchers hypothesized that torsional response is induced by eccentric distribution of stiffness, damping, or mass of a structure, or spatially non-uniform ground motion input to the long or large base mat of a structure. In this paper, we showed that the torque generated by horizontal displacement and perpendicular inertial force, which we call the *Q-Δ* effect, has an overlooked cause of torsional response. We formulated the equation of motion of a single finite-size mass–linear elastic shear and torsion spring and damper model, which is an idealized model of a building and revealed the resonance condition of torsional response to sinusoidal ground acceleration. Time-history response analysis was conducted and we verified that the torsional response forms a beat and the maximum torsional response of the simulation result agrees with that theoretically predicted. The model used had natural periods of 3.00 s and 4.00 s for the translational modes and 1.71 s for the torsional mode, which was predicted to cause torsional resonance, with 2% damping. The maximum torsional response reached 15.4°

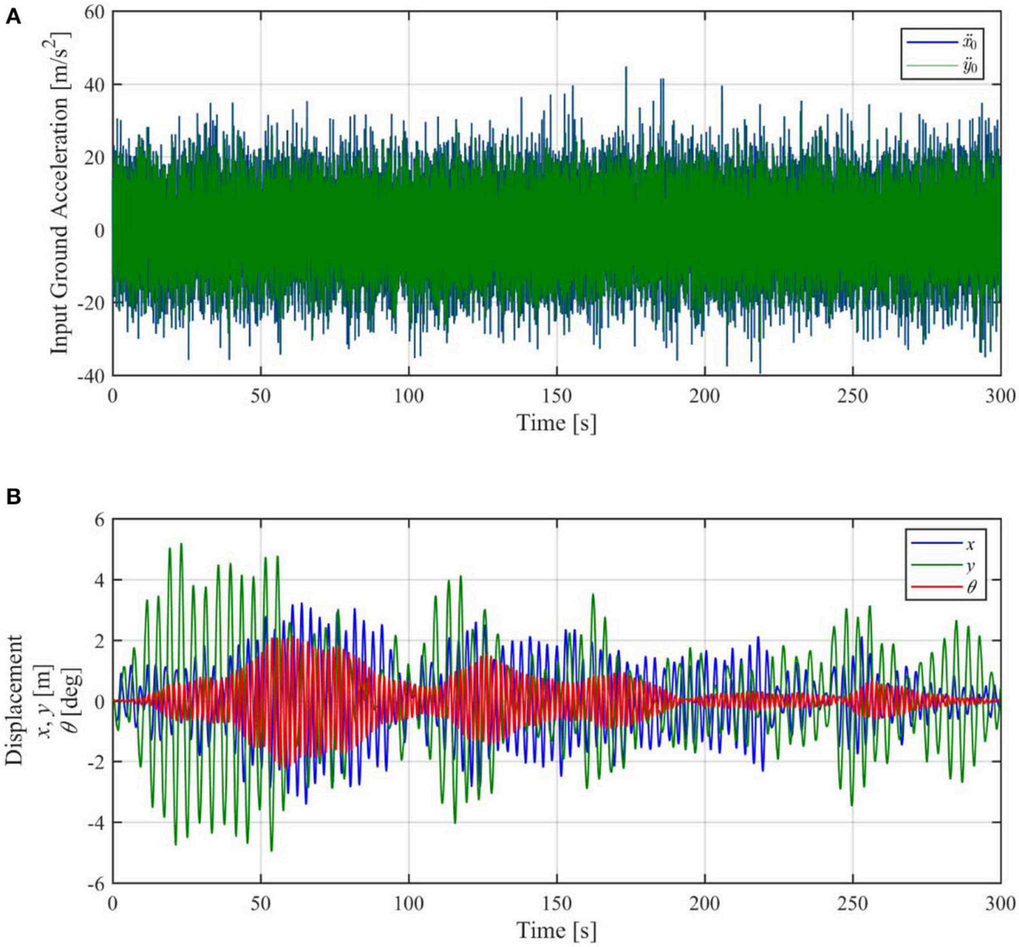

FIGURE 7 | Time-history analysis result of displacement response to one-directional (45° direction from the *x* axis) white noise ground acceleration. **(A)** Input ground acceleration, **(B)** Displacement response.

under two-directional sinusoidal ground accelerations with an amplitude of 1.00 m/s^2 and periods identical to the natural periods of the translational modes. We further conducted time-history response analysis of white noise ground acceleration and discovered that even one-directional white noise ground acceleration can induce the torsional response of a linear elastic system without any structural eccentricity. In this case, the torsional response exceeded 2.0° under the input white noise ground acceleration with a power spectrum density of 1.00 m^2/s^3.

Our future tasks are as follows:

- We have to expand the theory to a multi-story system and a system with structural eccentricity. In our theory, the natural frequency difference in two translational modes is necessary for induction of torsional response, and we have to check the necessity in consideration of higher modes.
- The maximum response should be estimated in a probabilistic manner and the prediction formula should be developed.
- We also have to expand the theory to a different input ground motion model, such as colored noise and non-stationary models.
- Further validation studies are also required, such as finite element analysis considering geometric nonlinearity and shaking table experiments.
- We also need to conduct a survey on the seismic damage risk of existing structures due to torsional response induced by the Q-Δ effect.
- The building code may need to be amended to consider the Q-Δ effect properly, and in this case, effective revision has to be studied.

AUTHOR CONTRIBUTIONS

MK constructed the theoretical framework. MK and HY derived the formulae and conducted the numerical simulation.

ACKNOWLEDGMENTS

This research was financially supported by a Japan Society for the Promotion of Science KAKENHI Grant Number 16H04455.

REFERENCES

Akiyama, H. (1984). P-Δ effects on seismic strength of multistory steel frames. *J Struct. Construct. Eng.* 340, 1–16.

Anagnostopoulos, S. A., Kyrkos, M. T., and Stathopoulos, K. G. (2015). Earthquake induced torsion in buildings: critical review and state of the art. *Earthquakes Struct.* 8, 305–377. doi: 10.12989/eas.2015.8.2.305

Antonelli, R. G., Meyer, K. J., and Oppenheim, I. J. (1981). Torsional instability in structures. *Earthquake Eng. Struct. Dyn.* 9, 221–237. doi: 10.1002/eqe.4290090304

Architectural Institute of Japan. (2000). *Damping in Buildings*. Tokyo: Architectural Institute of Japan.

Aschheim, M., and Hernández-Montes, E. (2003). The representation of P-Δ effects using Yield Point Spectra. *Eng. Struct.* 25, 1387–1396. doi: 10.1016/S0141-0296(03)00106-8

Basu, D., and Giri, S. (2015). Accidental eccentricity in multistory buildings due to torsional ground motion. *Bull. Earthquake Eng.* 13, 3779–3808. doi: 10.1007/s10518-015-9788-0

Bernal, D. (1987). Amplification factor for inelastic dynamic P-Δ effects in earthquake analysis. *Earthquake Eng. Struct. Dyn.* 15, 635–651. doi: 10.1002/eqe.4290150508

Cao, Y., Mavroeidis, G. P., Meza-Fajardo, K. C., and Papageorgiou, A. S. (2017). Accidental eccentricity in symmetric buildings due to wave passage effects arising from near-fault pulse-like ground motions. *Earthquake Eng. Struct. Dyn.* 46, 2185–2207. doi: 10.1002/eqe.2901

Cao, Y., Meza-Fajardo, K. C., Mavroeidis, G. P., and Papageorgiou, A. S. (2016). Effects of wave passage on torsional response of symmetric buildings subjected to near-fault pulse-like ground motions. *Soil Dyn. Earthquake Eng.* 88, 109–123. doi: 10.1016/j.soildyn.2016.04.001

Chandler, A. M., and Hutchinson, G. L. (1986). Torsional coupling effects in the earthquake response of asymmetric buildings. *Eng. Struct.* 8, 222–236. doi: 10.1016/0141-0296(86)90030-1

De la Llera, J. C., and Chopra, A. K. (1994). Accidental torsion in buildings due to base rotational excitation. *Earthquake Eng. Struct. Dyn.* 23, 1003–1021. doi: 10.1002/eqe.4290230906

Deierlein, G. G., Reinhorn, A. M., and Willford, M. R. (2010). *Nonlinear Structural Analysis for Seismic Design: A Guide for Practicing Engineers. NEHRP Seismic Design Technical Brief No. 4, NIST GCR 10-917-5*. Gaithersburg, MD: National Institute of Standards and Technology.

Falamarz-Sheikhabadi, M. R., and Ghafory-Ashtiany, M. (2015). Rotational components in structural loading. *Soil Dyn. Earthquake Eng.* 75, 220–233. doi: 10.1016/j.soildyn.2015.04.012

Flores, F., Charney, F. A., and Lopez-Garcia, D. (2018). The influence of accidental torsion on the inelastic dynamic response of buildings during earthquakes. *Earthquake Spectra* 34, 21–53. doi: 10.1193/100516EQS169M

Georgoussis, G. (2009). An alternative approach for assessing eccentricities in asymmetric multi-story buildings: 1. Elastic systems. *Struct. Design Tall Special Build.* 18, 181–202. doi: 10.1002/tal.401

Gičev, V., Trifunac, M. D., and Orbović, N. (2015). Translation, torsion, and wave excitation of a building during soil-structure interaction excited by an earthquake SH pulse. *Soil Dyn. Earthquake Eng.* 77, 391–401. doi: 10.1016/j.soildyn.2015.04.020

Goel, R. K. (2000). Seismic behaviour of asymmetric buildings with supplemental damping. *Earthquake Eng. Struct. Dyn.* 29, 461–480. doi: 10.1002/(SICI)1096-9845(200004)29:4<461::AID-EQE917>3.0.CO;2-6

Heredia-Zavoni, E., and Barranco, F. (1996). Torsion in symmetric structures due to ground-motion spatial variation. *J. Eng. Mech.* 122, 834–843. doi: 10.1061/(ASCE)0733-9399(1996)122:9(834)

Humar, J., Mahgoub, M., and Ghorbanie-Asl, M. (2006). Effect of second-order forces on seismic responses. *Can. J. Civil Eng.* 33, 692–706. doi: 10.1139/l05-119

Jennings, P. C., and Bielak, J. (1973). Dynamics of building-soil interaction. *Bull. Seismol. Soc. Am.* 63, 9–48.

Karayannis, C. G., and Naoum, M. C. (2018). Torsional behavior of multistory RC frame structures due to asymmetric seismic interaction. *Eng. Struct.* 163, 93–111. doi: 10.1016/j.engstruct.2018.02.038

Lin, J. L., and Tsai, K. C. (2007). Simplified seismic analysis of one-way asymmetric elastic systems with supplemental damping. *Earthquake Eng. Struct. Dyn.* 36, 783–800. doi: 10.1002/eqe.653

MacRae, G. A. (1994). P-Δ effects on single-degree-of-freedom structures in earthquakes. *Earthquake Spectra* 10, 539–568. doi: 10.1193/1.1585788

Moghadam, A. S., and Aziminejad, A. (2004). "Interaction of torsion and p-delta effects in tall buildings," in *Proceedings of 13th World Conference on Earthquake Engineering* (Vancouver, BC).

Pekau, O. A., and Syamal, P. K. (1984). Non-linear torsional coupling in symmetric structures. *J. Sound Vibrat.* 94, 1–18. doi: 10.1016/S0022-460X(84)80002-4

Rutenberg, A. (1982). Simplified p-delta analysis for asymmetric structures. *ASCE J. Struct. Div.* 108, 1995–2013.

Stathi, C. G., Bakas, N. P., Lagaros, N. D., and Papadrakakis, M. (2015). Ratio of Torsion (ROT): An index for assessing the global induced torsion in plan irregular buildings. *Earthquakes Struct.* 9, 145–171. doi: 10.12989/eas.2015.9.1.145

Tremblay, R., Côté, B., and Léger, P. (1999). An evaluation of P-Δ amplification factors in multistorey steel moment resisting frames. *Can. J. Civil Eng.* 26, 535–548. doi: 10.1139/l99-015

Tso, W. K. (1975). Induced torsional oscillations in symmetrical structures. *Earthquake Eng. Struct. Dyn.* 3, 337–346. doi: 10.1002/eqe.4290030404

Uetani, K., and Tagawa, H. (1992). Deformation concentration phenomena in the process of dynamic collapse of weak-beam-type frames. *J. Struct. Const. Eng.* 483, 51–60.

Veletsos, A. S., and Meek, J. W. (1974). Dynamic behaviour of building-foundation systems. *Earthquake Eng. Struct. Dyn.* 3, 121–138. doi: 10.1002/eqe.4290030203

Wilson, E. L., and Habibullah, A. (1987). Static and dynamic analysis of multi-story buildings, including p-delta effects. *Earthquake Spectra* 3, 289–298. doi: 10.1193/1.1585429

Wynhoven, J. H., and Adams, P. F. (1972). Behavior of structures under loads causing torsion. *ASCE J. Struct. Div.* 98, 1361–1376.

Yu, B., Yang, L. F., and Li, B. (2015). P-Δ effect on probabilistic ductility demand and cumulative dissipated energy of hysteretic system under bidirectional seismic excitations. *J. Eng. Mech.* 141, 1–16. doi: 10.1061/(ASCE)EM.1943-7889.0000864

Conflict of Interest Statement: The authors declare that the research was conducted in the absence of any commercial or financial relationships that could be construed as a potential conflict of interest.